TWIP Steels: Mechanical and Metallurgical Properties - A Review

Víctor Alcántara Alza
Mechanical Engineering Department
National university of Trujillo
Trujillo-Perú
Victoralc_unt@hotmail.com

Abstract— This document reviews the recent development of one of advanced steels very used in the automotive industry; Steels with Twinning induced by plasticity named, TWIP steels. Its composition consists of: high manganese (Mn) and low carbon (C) and, some cases alloyed with small amounts of Si, Al or Nb, which makes them austenitic steels at room temperature. When subjected to high rates of deformation they can achieve a combination of high mechanical strength and elongation and can reach values even greater than 1 GPa and large elongations up to more than 60%, which make them attractive for use in the manufacture Auto body parts in the automotive industry. The review is divided into two parts. First they are studied the twinning mechanisms of these steels, analyzing the various influencing factors, emphasizing the stacking fault energy (SFE) and its effect on the deformation hardening mechanism, as well as the phases that occur due to the variation of the strain rate, showing results at optical and electron microscopy level. Then its tensile mechanical properties are presented and explained, based on metallurgical analysis, and the influence of the other factors involved are analyzed. In summary: From all the literature reviewed, it is concluded the twinning and dislocation mechanisms are decisive and explain why an increase in mechanical strength is accompanied by an increase at deformation.

Keywords— Austenite; Twin; Microstructure; high manganese steels; Stacking Fault.

I. INTRODUCTION

In the last decades, Investigations were directed at the automotive industry in order to obtain much lighter car bodies to reduce fuel consumption costs. Thus appeared light steels with the combined effect of high mechanical strenght and high ductility known as AHSS advanced steels with various combined effects of strength and ductility. One of the latest versions of these is: the twinning-induced transformation steels, called TWIP steels. Nowadays, more and more attention is paid to research related to the design of its composition, the improvement of the properties and the deformation mechanism [1], [2], [3], [4].

TWIP steels are austenitic manganese steels at room temperature, highly ductile and high-strength, which have the property that when deformed they generate strain-hardening twins, which prevent the movement of dislocations and nucleate and increase as the rate of deformation increases [5], [6], [7].

The chemical composition of these steels is basically made up of Mn and C, in the range: (15% - 30%) Mn and (0.5%-1%)C. Mn is a strong austenite phase former; with a content of 22% to 35%, the material has a stabilized austenitic phase. The Al Si or Nb microalloys help to obtain greater mechanical strenght and a high uniform elongation; a phenomenon that is associated with twinning. Si and Al are elements that help to achieve a totally stable austenitic microstructure.

the plastic deformation occurs through twinning, which is said to improve elongation. Continuous twin boundary formation can impede dislocation movements to improve strength [8]. The twins, decrease the grain size and hinders the dislocation movement during deformation, improve the strength of TWIP steel [9], [10], [11], [12]. In addition, these twins, on the one hand, cause a high degree of strain hardening, preventing the movement of dislocations within the grain, but on the other hand, since the austenitic grain is ductile, the sliding mechanisms improve the ductility of TWIP steel [13].

TWIP steels have a great elongation capacity that can reach up to 50% for a mechanical resistance of 1000 MPa or even 35% for 1400 MPa. It is the first time that a steel offers such extreme properties. This material is specially adapted to lighten automotive structure parts and thus contribute to the reduction of greenhouse gases.

Contemporary TWIP steels exhibit high ultimate tensile stresses along with exceptionally large tensile elongations (60%) over a wide range of strain rates (10-3-103s-1). The importance of TWIP steels as innovative structural materials cannot be underestimated, as the TWIP steel concept has also opened up the possibility of creating new steel grades with a wide range of properties. These developments have already been addressed in the literature [14], [15], [16], [17].

In conventional TWIP steels, the carbon content is normally kept below 0.3%C, to avoid carbide precipitation. Moreover, Mn reduces the precipitation temperature of cementite. [18]. Recent experiments

have shown that the tensile strength and elongation of TWIP steels could reach up to 1200 MPa and 90% elongation respectively **[19], [20].**

Even though these steels have remarkable mechanical properties due to the high rate of strain hardening. However, the yield stresses (YS) at TWIP steels with different grades

are less than 400 MPa **[21], [22], [23] [24] [25], [26]**. This limits the immediate application of TWIP steels in the automotive industry. Various studies have tried to improve the YS. Methods include reducing grain size to a few microns **[27], [28]**; the precipitation of carbides of V, Ti, Nb **[29],** partial recrystallization **[30];** and so on. It is a great challenge to improve the YS without compromising ductility.

The present study aims to carry out a review study based on specialized literature, to determine which are the mechanisms of the twinning process, that allow TWIP steels simultaneously present high mechanical resistance and high elongation.

II. PRELIMINARY REVIEW

2.1. Twinning process.

The study of dislocations and substructures of the twins is key to obtain a better understanding of the mechanisms of strain hardening and, therefore, of the mechanical properties.

Twinning is a movement of planes of atoms in the lattice, parallel to a specific twinning plane, so that the lattice is divided into two differently oriented symmetrical parts. The amount of movement of each plane of atoms in the twinned region is proportional to its distance from the twinning plane, so that a mirror image is formed across the twinning plane, as shown in the following figures 1 y 2
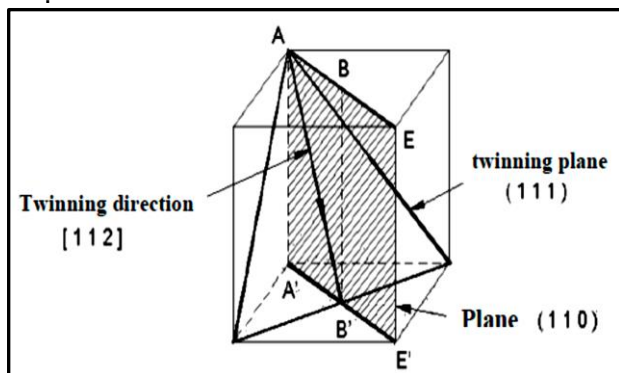
.

Fig.1. Diagram of a twinning plane and twinning direction in a body centered cubic lattice b.c.c.

Among the three most common crystalline structures in metals bcc, fcc and hcp, the compact hexagonal structure hcp is the most prone to forming deformation twins when the material is deformed due to its small number of sliding systems.
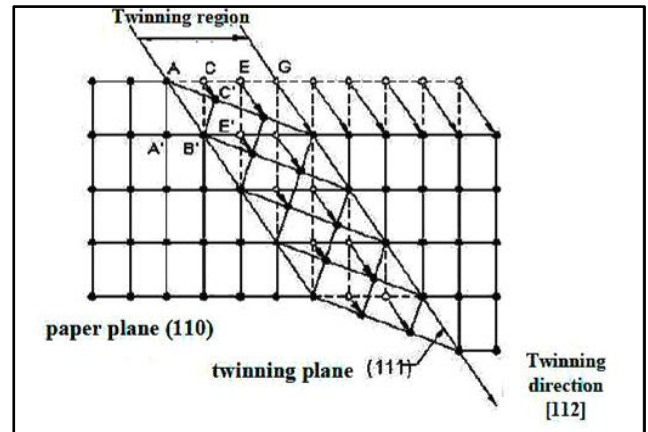

Fig. 2. Schematic diagram of twinning in a lattice b.c.c.

In Fig.1, a centered-body cubic lattice bcc, is observed. Twinning plane (111) intersects plane (110) along line AB', which is the twinning direction. Figure 2 shows the twinning mechanism. The plane of the paper is (110) and many unit cells are taken together. Each plane (111) in the twinning region moves tangentially to direction [112]. The first, CD, moves a third of an interatomic distance; the second, EF, moves two-thirds of an interatomic distance; and the third, GH, moves a whole space.

The twinning mechanism of Fig. 2 can be better understood with the following explanation. If a line is drawn from atom A' perpendicular to the twinning plane AB, there will be another C' atom, exactly the same distance from the twinned plane, on the other side. The same is true for all atoms in the twinned region, so that you actually have a mirror image in the twinned region that reflects the non-twinned portion of the crystal. As the atoms end up in interatomic spaces, the orientation of the atoms has been changed by the distance between them. The plane and direction of twinning are not necessarily the same as that of the sliding process. In b.c.c metals, the twinning plane is (111) and the twinning direction is [112]

2.2. Twin formation.

Twins can be generated by atomic displacements produced by strain (mechanical twins) and also during post-strain annealing heat treatments (annealing twins).

Twins are formed as a result of shear stress applied in a direction parallel to the twinning plane and remaining in the twinning direction. The component of axial stress, normal to the twinning plane, is not important in the formation of the twin. Contrary to sliding, the shear stress required to be able to form a twin is not invariant with respect to the twinning plane, but different values may be required over a fairly wide range.

The twins are formed only in metals that have undergone previous deformation by sliding, and the necessary condition for the nucleation of twins is

justified: preventing the sliding process, forming barriers that prevent the movement of dislocations in certain restricted areas.

Twin growth is primarily a function of the stress required for their nucleation, it works in the following ways: a) If twins are nucleated at very low stresses, the stress required for their growth will be of the same order of magnitude as the nucleation stress, b) If twins are formed under conditions that result in very high stress levels prior to nucleation, the growth stress can

be much less than nucleation. When this happens, the twins grow very quickly, as soon as they are nucleated.

The twins behave like grain joints gradually reducing the effective sliding distance of the dislocations, which results in a dynamic Hall-Petch effect as can be observed in Fig. 3, Twin joints result in a very high hardenability and extraordinary energy absorption in case of impact [31].
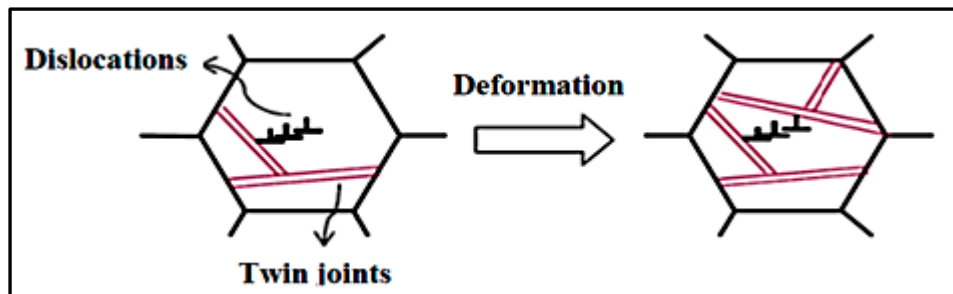

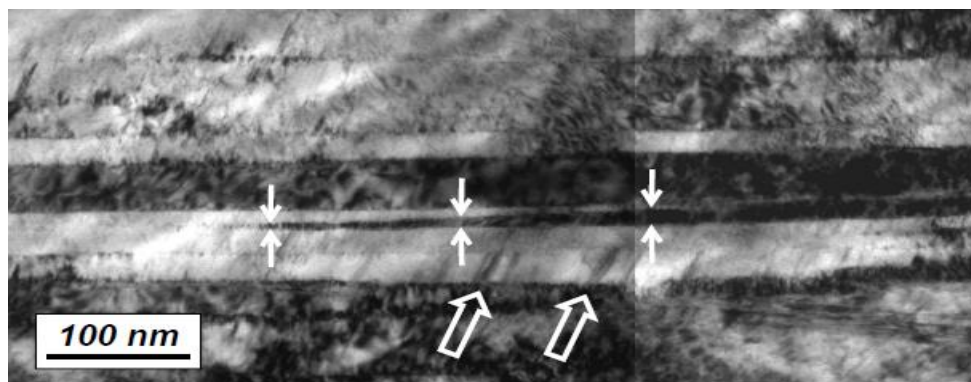**Fig. 3**. Dynamic Hall-Petch effect due to the twin joints present in TWIP steels.

Fig. 4. TEM micrograph of TWIP steel with Fe-18% Mn-0.6% C. highly deformed. Small white arrows indicate a twin thickness less than 50 nm. The large arrows indicate stacking faults in the matrix.

In Fig. 4 we have a TEM micrograph of TWIP steel with Fe-18% Mn-0.6% C highly deformed, where it is possible to observe a twins thickness ~ 50 nm and the stacking faults between twins [38].

2.3. Stacking Fault Energy (SFE)

A stacking fault is a disruption of the normal stacking sequence of atomic planes in a compact crystal structure. These interrupts carry a certain so-called stacking fault energy (SFE). This energy plays a key role in the deformation mechanisms of austenitic steels; deformation mechanisms induced by transformation or twinning such as that produced in TWIP steels. Therefore, a brief summary will be dedicated to indicate how the parameters that determine the SFE and their relationship with mechanical twinning influence.

A stacking fault is formed by the dissociation of a perfect dislocation into two Shockley partials. SFE is determined by the distance between partial

dislocations: a low SFE corresponds to a high distance between partial dislocations [32]. The width of the stacking fault is a consequence of the balance between the repulsive force between two partial dislocations on the one hand and the attractive force due to the surface tension of the stacking fault on the other hand. Therefore, the equilibrium width is partially determined by the stacking failure energy. When the SFE is high, dissociation of a complete dislocation into two partials occurs, which is energetically unfavorable and the material can be deformed by dislocation slip or cross slip. Lower SFE materials exhibit wider stacking faults and have a more difficult cross-sliding. The SFE modifies the ability of a dislocation in a crystal to slide on an intersecting sliding plane. When the SFE is low, the mobility of dislocations in a material decreases [33].

High SFE materials deform by sliding from complete dislocations. Because there are no stacking failures, screw dislocations can slip. It was found that cross-slip occurs under low stress for high SFE

materials like aluminum. This gives the metal additional ductility because with cross sliding it only needs three other active sliding systems to undergo high stress. **[34], [35].** This is true even when the lattice is not ideally oriented. Therefore, high SFE materials do not need to change orientation to accommodate large deformations due to cross slip. Some reorientation and texture development will occur as the grains move during deformation. Extensive transverse sliding due to large deformation also causes some grain rotation **[36].** However, this reorientation of grains in materials with high SFE content is much less frequent than in materials with low SFE content.

The governing parameters of the microstructure of TWIP steels are: fault energy relatively low (SFE ≤ 20 mJ/m^2) which favors the transformation:

$$\gamma(fcc \text{ (austenite)} \rightarrow \varepsilon(hcp \text{ martensite}) \qquad (1)$$

However, for SFE of 25mJ/m2 (>20 mJ /m2) be causes a mechanical twinning in a stable solid solution of γfcc **[76],** [**77**]**.**

After analyzing the effect of alloying agents and other factors that affect the deformation of TWIP steels; came to the following conclusion: The fundamental principle of the microstructural design of TWIP steels is as follows: The alloying elements must provide SFE values ranging between 20 and 40 mJ/m^2 **[37].** However, studies on the deformation mechanism in TWIP steels have not yet answered two basic questions: (1) Why does the martensitic transformation for a given TWIP steel gradually replace the deformation twinning with a decreasing deformation temperature? (2) Why do TWIP steels with different composition exhibit different deformation behaviors, such as the TRIP effect and / or dislocation slip, which in turn change the microstructure at a given temperature?

2.4. Twinning Hardening Mechanisms

Twinning is a hardening process that is always associated with sliding, therefore it cannot be considered independently. This means that it must be considered as a secondary mechanism to sliding, and the hardening that it achieves must be the consequence of multiplying the actions of the sliding hardening. In this sense, it is justified that twins increase hardening for the following reasons: a) They divide the grains size into three parts, with the incidence that have the grain size. b) It blocks the dislocations that were acting on the single crystal at that time with the consequent inhibition of sliding. c) It hinders the movement of grain edges due to the compression resistance imposed by the twin when the grain tends to stretch. Consequently, twinning is a hardening mechanism that enhances the inhibition of plastic flow by sliding, by partitioning the grain and blocking the edges.

III. TWINNING PROCESS IN TWIP STEELS

3.1 Mechanical twins and annealing twins.

Twins can be generated by atomic displacements produced by strain (mechanical twins) and also during post-strain annealing heat treatments (annealing twins).

Plastic deformation occurs on a sample of TWIP steel, performing an analysis of the microstructure represented in Fig. 5, where twins are observed. The twins are identified within the microstructure as narrow sub-grains with quite rectilinear and parallel edges that divide the initial single crystal, presenting the following characteristics:
a) The twin has the same composition and structure of the grain in which it is immersed, b) The twinning speed is very high, c) It usually happens when the specimen has suffered certain levels of glide,
d) Each twin that is formed forces higher elevations of the applied stress in order to increase the deformation.

Twinning is a mechanism, complementary to sliding, by which the alloy is hardened in the same way as it happened with sliding.

In a TWIP steel there is no phase transformation during cooling or deformation, but the orientation of part of the austenite will change due to mechanical twinning. This different behavior of austenite is attributed to its stacking fault energy SFE **[40].** Like all defects, a stacking fault causes a change in the structure.
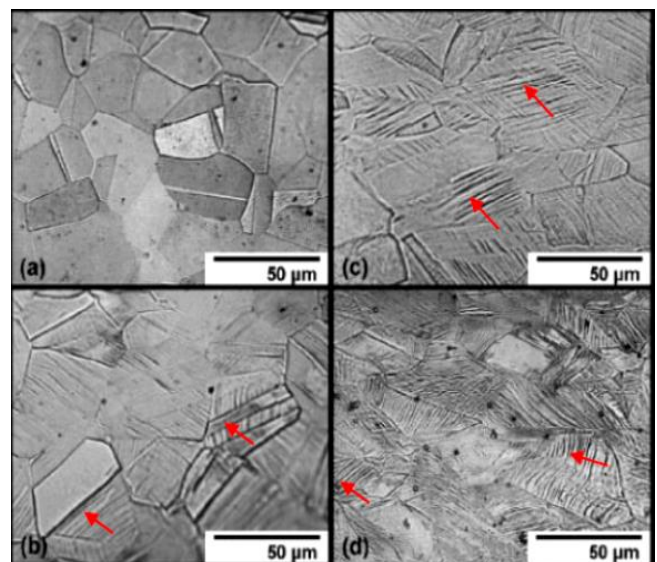

Fig. 5. Optical micrographs of typical TWIP steel (a) no strain, (b) 18% strain, (c) 26% strain, (d) 34% strain. The red arrows indicate twins.

As the strain increases, the density of strain twin increases **[39].** As the SFE decreases, the faults become wider and the transverse sliding more difficult, so that mechanical twinning is becoming the preferred deformation mode **[41].**

The energy required for the production of twins is denoted as: γSFE (J./m^2) changes with the alloy

composition and the strain temperature. Its magnitude controls the ease of cross-sliding of the dislocations and therefore different mechanisms can be activated at different energy stages, called stacking fault energy (SFE).

3.2. Stacking fault energy (SFE) in TWIP steels

The defining characteristic of TWIP steels is the small magnitude of the intrinsic SFE. In addition to limiting the rate of dynamic recovery, the low stack fault energy of TWIP steels results in the formation of isolated stack fault and deformation twins, reducing the mean free path of dislocations. Both effects lead to an increase in the strain hardening rate **[42].**

The main objective of SFE studies for TWIP steels is to determine the range of SFE values in which austenite is susceptible to extensive mechanical twinning. Frommeyer et all, **[71],** demonstrated that for SFE values ≤16 mJ / m^2, the hexagonal ε-martensite is formed, while for SFE values greater than 25 mJ / m^2 a completely austenitic structure is retained after plastic stress intense and the appearance of the twinning after a little effort. Allain et al., **[72]** found that mechanical twinning becomes the dominant deformation mechanism in the SFE range: 12-35 mJ/m^2. At higher SFE values, no mechanical twinning occurs. Strain induced ε-martensite appears with lower SFE, while in the SFE range: 12-18 mJ/m^2, mechanical twinning and martensitic transformation occur sequentially. Strain twinning promotes ε-martensite formation. The thickness of ε- martensite plates and the deformation twins are almost equal and can vary from 20 to 40 nm.

Due to the difficulty of measurement, there are no experimental SFE values for most TWIP alloy systems, but there are a considerable number of theoretical calculations **[73], [74], [75].** The critical region of stacking defects to achieve twinning-induced plasticity is still uncertain.

3.3. Deformation micro-twins in TWIP steels

A very important characteristic of TWIP steels is their deformation mode; As previously mentioned, in addition to the classic dislocation sliding mechanism, these steels are also deformed by the twinning mechanism, but the twins can be micrometric visible with optical microscopy or nanometric visible with transmission electron microscopy, as shown in Fig. 6, where the boundaries of the twin behave as obstacles to the movement of the dislocations, in a similar way to the grain boundaries **[43].** The more it deforms, the density of the twin boundary increases. The instantaneous hardening coefficient n is kept at a high level (n> 0.45) and the structure is finer and consequently the neck formation of the specimen from a tensile test is relegated to a greater amount of deformation.

The interaction between dislocations, grain boundaries, stack fault, and strain twins results in sustained high strain hardening during the deformation

process. However, the defining characteristic of TWIP steels is the small magnitude of the intrinsic stacking energy; since in addition to limiting the dynamic recovery rate, the low stack fault energy of TWIP steels results in the formation of isolated stacking fault and strain twins, which reduces the mean free path of dislocations. Both effects lead to an increase in the strain hardening rate **[44].**
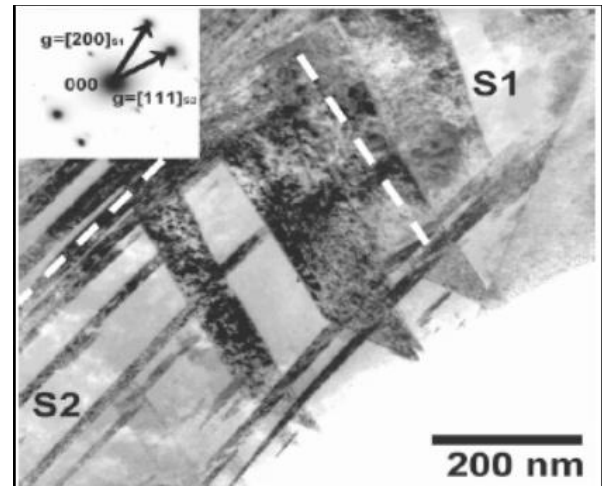

Fig.6. Micrograph (TEM) of a TWIP steel sample deformed at room temperature. Micro twins appear dark and two twinning systems (short dashed lines)

IV. PHASES AND MICROSTRUCTURES

Manganese is the main alloying element of TWIP steels that provides a generation of austenitic structure **[45].** But any Mn content does not generate the austenitic structure that TWIP steels need. With a low and medium content of Manganese, of (5% - 10%), two types of microstructure appear (ferrite and austenite). As the manganese content increases up to 22%, the material consists of two type microstructures: austenite and martensite. For higher Mn contents (30-35% Mn) the structure becomes totally austenitic **[46].** A manganese content greater than 20%wt favors the formation of a compact hexagonal ε- martensite phase (hcp), while an intermediate of manganese content 15% wt promotes the formation of both variants of hexagonal ε- martensite. and α´cubic martensite.

Fig. 7 shows the microstructure difference in high Manganese and medium Mn TWIP steels **[47].** In both cases, its high ductility is achieved by activating the mechanical twinning mechanism that improves plasticity (TWIP effect) during deformation. Medium Mn steel has an ultra-fine grain ~ 500 nm, and austenitic-ferritic microstructure. Its ductility is controlled by the activation of the deformation-induced transformation mechanism that increases plasticity (TRIP effect) or a combination of the TWIP and TRIP effect that occurs in succession.

Fig. 8 shows the microstructure of a sample annealed at 650 °C of the TWIP Fe-20Mn-0.045C-3Si-3Al steel is presented at an optical level **[78].** It is observed that the matrix presents mixed grains and many annealing twins. A greater number of twins can

be obtained with a lower annealing temperature as long as the time is not adequate for recovery. The microstructure shows equiaxed grains with numerous annealing twins in an austenite matrix. Diffraction analyzes indicate that most of the grains are austenitic in phase. The results suggest that the average grain size is ~ 8 μm, and the fraction of grain boundaries with a disorientation angle > 15°.
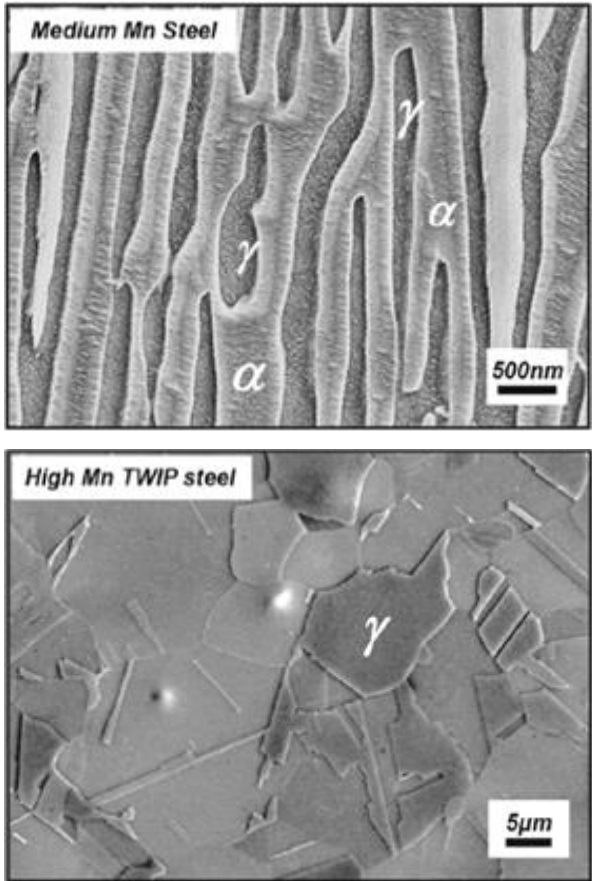

Fig. 7. Comparison of the high and medium Mn TWIP steel microstructure. High Mn steel is fully austenitic and medium Mn steel has an ultrafine grain austenitic-ferritic structure.
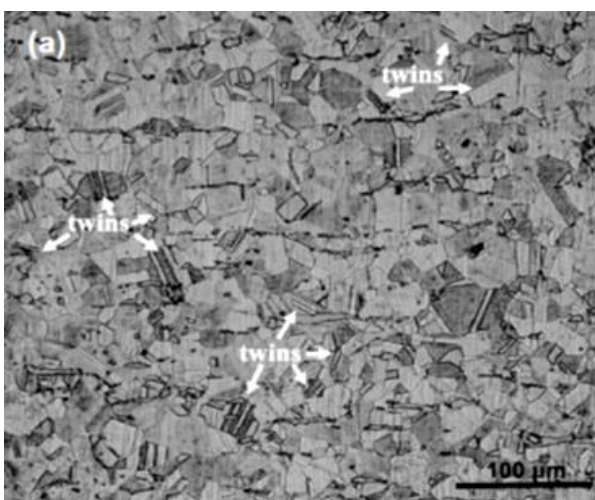

Fig. 8. Morphology obtained from the annealed 20%Mn, 3%Si, 3%Al, 0.045%C steel sample before being deformed.

Fig. 9. (TEM), shows that the number of twins/ ε-martensite laths, in the samples at a strain level of 18% (910 MPa). **[78].** The laths of the cubic martensite α´ can be observed at the intersections of the twin and / or hexagonal ε-martensite bundles. Twin thicknesses are observed at nanometric scales.
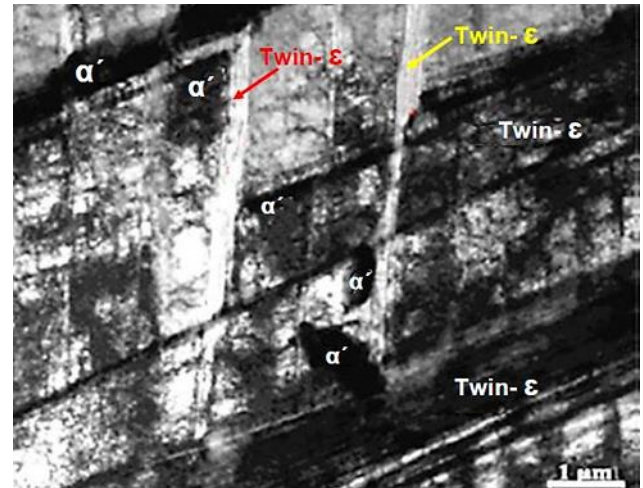

Fig. 9. TEM image of the annealed 20Mn–3Si–3Al–0.045C steel at the strain of 18%. The microstructure shows twins, ε-martensite, and α´-martensite.

Figure 10 shows at optical level the effect of manganese content on the microstructure can be observed, where the density of twins formed highlights according to the percentage of applied deformation **[49].**
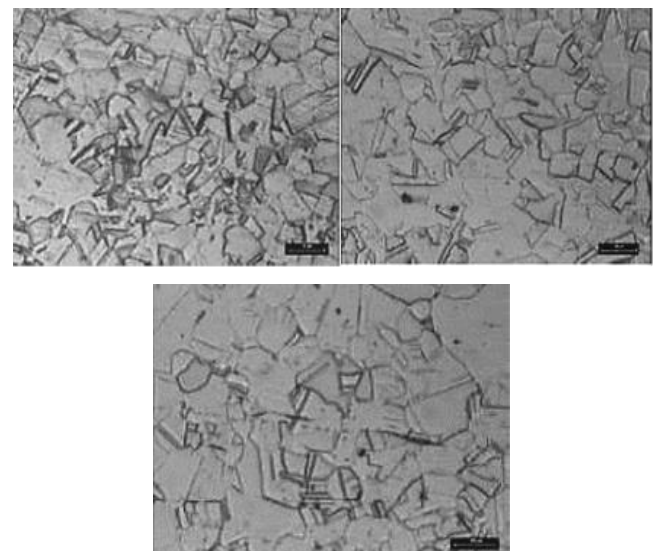

Fig. 10. TWIP steel Microstructures at different manganese contents: (a) 22%, (b) 24%, (c) 26%. High twin densities are observed according to the high manganese content.

4.1. Effect of the Deformation Rate on the Microstructure of TWIP steels.

In TWIP steel, deformation occurs by dislocation and twinning movement which in turn depends on the rate of deformation. The TWIP effect is believed to be mainly due to a dynamic Hall-Petch effect.

Table 1 shows the phases that form before and after subjecting the samples of the various TWIP steels to a uniaxial stress strain test at room temperature **[50].**

Table 1. Chemical analyses and the constituent phases before and after tensile testing at 10^{-4} s^{-1} at room temperature.

| Steel	Chemical composition, mass.%					Phases before tensile test	Phases after tensile test
	Mn	Si	Al	C	Fe		
Fe-15Mn-4Si-2Al	16.2	4.0	1.8	0.02	Bal.	$\gamma + \alpha + \varepsilon$	$\gamma + \alpha' + \varepsilon + \alpha$
Fe-15Mn-3Si-3Al	17.9	3.2	2.9	0.02	Bal.	$\gamma + \alpha$	$\gamma + \alpha' + \alpha$
Fe-15Mn-2Si-4Al	15.9	1.9	3.5	0.01	Bal.	$\gamma + \alpha$	$\gamma + \alpha' + \alpha$
Fe-20Mn-4Si-2Al	18.2	4.3	1.8	0.06	Bal.	$\gamma + \alpha$	$\gamma + \alpha' + \varepsilon$
Fe-20Mn-3Si-3Al	20.1	2.8	2.9	0.04	Bal.	$\gamma + \varepsilon$	$\gamma + \alpha' + \varepsilon$
Fe-20Mn-2Si-4Al	18.1	1.8	3.5	0.03	Bal.	$\gamma + \alpha$	$\gamma + \alpha + \alpha'$
Fe-25Mn-4Si-2Al	25.5	3.9	1.8	0.03	Bal.	$\gamma + \varepsilon$	$\gamma + \varepsilon$
Fe-25Mn-3Si-3Al	26.6	3.0	2.8	0.03	Bal.	γ	γ
Fe-25Mn-2Si-4Al	25.6	2.0	3.8	0.03	Bal.	γ	γ
Fe-30Mn-4Si-2Al	28.7	4.0	2.0	0.02	Bal.	$\gamma + \varepsilon$	$\gamma + \varepsilon$
Fe-30Mn-3Si-3Al	29.2	3.0	2.8	0.02	Bal.	$\gamma + \varepsilon$	γ
Fe-30Mn-2Si-4Al	30.6	2.0	3.9	0.01	Bal.	γ	γ
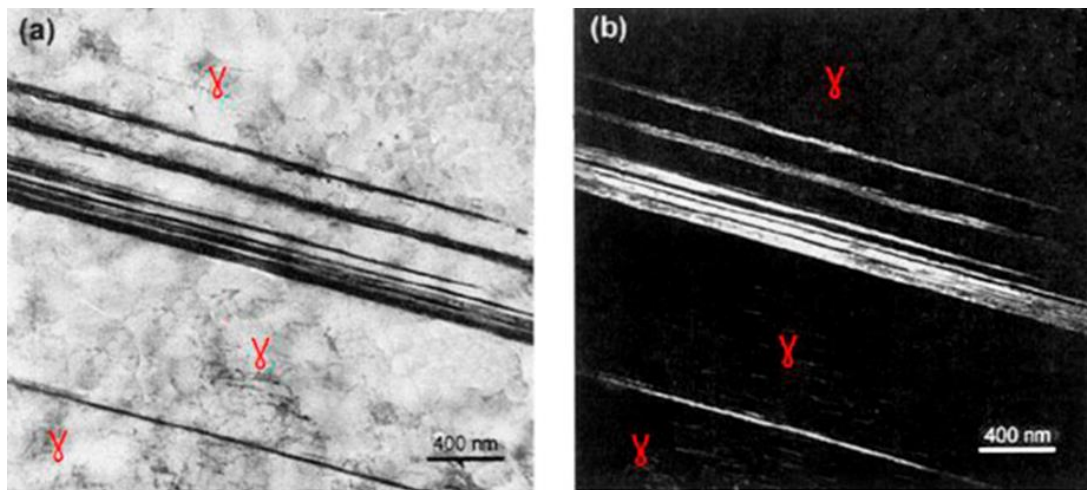
Fig. 11. TEM images of the at room temperature deformed sample (ε=10%); (a) bright field image (b) dark field image (Fe-25%Mn-3%Si-3%Al). The image is the steel indicated with the red arrow.

Table 1 shows the phase constitution before and after a stress test at room temperature of high and medium Mn TWIPS steels. To achieve the austenite phase stable at room temperature, which is characteristic of TWIP steels, while maintaining a manganese content of less than 27% by weight; it becomes necessary to suppress the formation; both of the cubic martensite α' and of the martensite "ε". This is achieved by adding carbon to the alloy. A carbon addition of 0.6% by weight is sufficient to obtain a uniform carbide-free austenite microstructure, avoiding the formation of martensite **[48].** An alternative approach to acquiring a stable fully austenitic microstructure is to use higher manganese contents, avoiding the additions of carbon. In this case, silicon and aluminum are added instead of carbon as can be seen in Fig. 11. **[50]**

Since strain twinning is a phenomenon that comes from a dislocation mechanism, the difference in twin morphology and volume fraction at different strain rates may be due to a process based on dislocation. At high rates of deformation, dislocations will have less time to wait on obstacles to gain enough heat energy to overcome an obstruction.

The tension required to generate twins, known as "twinning stress", can be considered to be a combination of two separate aspects. First, a strain is required for twin nucleation followed by an additional strain for twin growth, which together define the twinning stress. However, to determine the stress required to nuclear a twin experimentally, it is extremely difficult **[79].** Consequently, it is generally considered that the cores for twins already exist within the material, due to stacking faults, and that the

twinning stress that is experimentally determined is actually the stress required for the growth of the twins. This means that the nucleation or growth of the twin occurs when the external shear stress through the K1 plane resolved in direction 1, reaches a critical value, similar to "Schmid's law" for sliding.

Fig. 12 shows the microstructure of TWIP steel: cold rolled Fe-22Mn-0.6C with a 50% reduction and then annealed at 500 °C for 3600 s. The microstructure shows a high density of deformation twins. The results of the uniaxial tensile tests can be seen in Figure 13, which shows that the tensile behavior is quite isotropic after annealing, and that the yield strength has decreased from the total hardness value of 1600 MPa to 1200 Mpa **[14]**. Uniform elongation increases from 2% to more than 8% due to increased work hardenability. Therefore, a recovery and recrystallization treatment at a temperature below 625 ° C could provide an interesting combination between YS and work hardening.
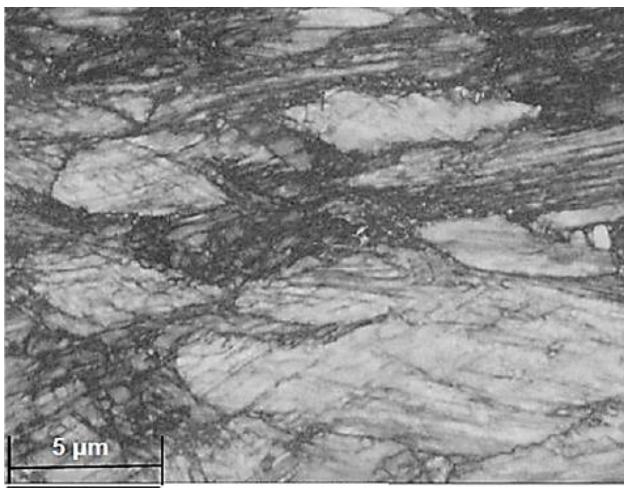

Fig. 12 SEM image of microstructure in TWIP steel (Fe–22Mn–0.6C) after 50% cold reduction and a recovery treatment at 500 °C for 1 h**.**
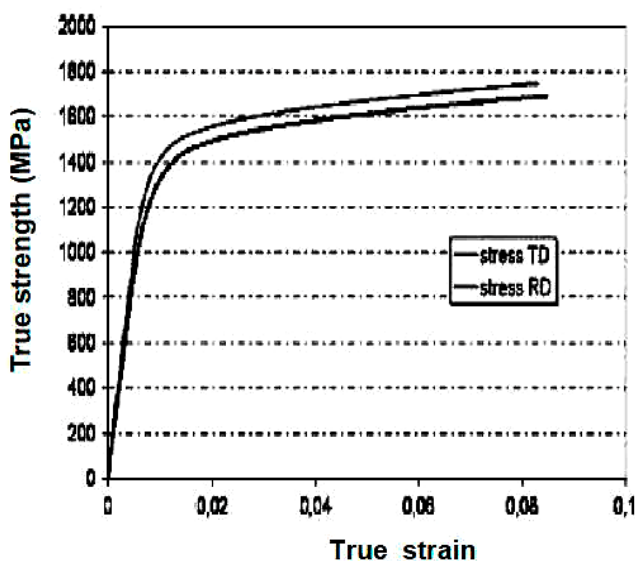

Fig. 13. Tensile behaviour of Fe–22%Mn–0.6%C after 50% cold reduction and a recovery treatment at 500 °C for 1 h; RD: rolling direction, TD: transverse direction.

Figure. 14 shows at optical level, the effect of strain rate on the microstructure of the Fe-15Mn-2Al-2Si-0.7C, TWIP Steel. The microstructure shows the presence of shear bands with a 45° inclination. The presence of bands increases with the higher deformation rates, which shows that these shear mechanisms at high rates of deformation are as important as sliding and twinning. The origin of these bands generally appear where there is a high density of dislocations. All the microstructures presented in this figure demonstrate that a strain twinning occurs within the material for all strain rates tested **[51]**.

Fig.15. shows TEM micrographs revealed that high density deformation twin forms during the deformation for different strain rate. The microstructure shows that width of deformation twin lath decreases as the strain rate increases. **[52]. In** Fig. 15 (a) shows Twip steel in the annealed state, not deformed with 1000 nm (1 µm) as indicated by the scale in the figure; These Twins are the so-called thick annealing twins. In Figs. (b, c, d) shows the presence of deformation twins whose thickness is at nanometric scale, which decrease as the deformation rate increases. The deformation twins of Fig. 15 (b) has thicknesses ~ 80 nm, and then follows the observed in Fig 15 (c), which is the most observable, with a thickness of 50 nm. Finally, in Fig. 15 (d) the deformation twins appear in the form of fine little measurable traces in the figure.

IV.2. Complements on deformation twins

The sliding that stress produces along planes between rows of atoms within the crystal structure can deform them plastically. This can take the form of a slip. The twins thus formed were called "sliding twins" or "deformation twins". A non-twinned crystal exists in a lower energy state. Higher energy is expected if the material is subjected to double sliding. The energy is provided as part of the work of distorting the crystal. In contrast, crystals that develop twins during growth in some cases achieve a lower energy state. However, the sliding twins were previously at a minimum

The high energy of the twins is confined near the limit of the twins. This energy is a surface or interfacial energy. The joints between sliding twins are flat due to the different sliding progression. However, these sliding twins can bend if the crystal lattice is twisted.

When a crystal is generated by twin slip, it does so in an unusual way and the process usually shows different results from its manifestation. If a stress that has a shear component in the sliding plane is exerted on the glass and is strong enough to overcome the barriers, all parallel planes of the glass are subject to stress, but sliding does not occur at all planes simultaneously.

A cristal plastically generated by sliding is characterized by numerous parallel lamellae called bands of parallel twins. This repetitive twinning is

essentially a polysynthetic twinning. Lamellar distribution can be regular or irregular depending on the diffusion and under special conditions. The widths of the bands depend on the extent of the deformation and distribution of these special conditions that cannot be predicted.

Twinning significantly changes the deformation behavior of the parent grain. The twin creation divides the grain into two domains. The first domain tends to deform elastically under greater deformation, while the other undergoes a plastic deformation by prismatic sliding. This behavior has been observed in compact structures fcc and hcp not only in TWIP steels but also in other metals.
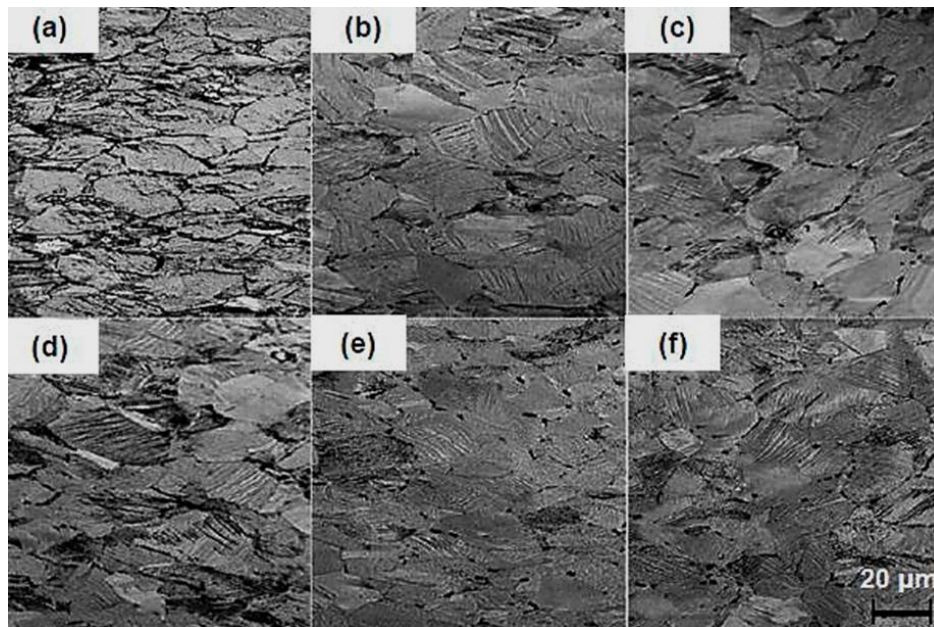

Fig. 14. Optical micrographs showing the effect of strain rate on the microstructure of the. (Fe-15Mn-2Al-2Si-0.7C,) TWIP steel, in a tensile test up to failure. (a) $0.003s^{-1}$, (b) $0.1s^{-1}$, (c) $233s^{-1}$, (d) $1473s^{-1}$, (e) $1600s^{-1}$, (f) $1934s^{-1}$
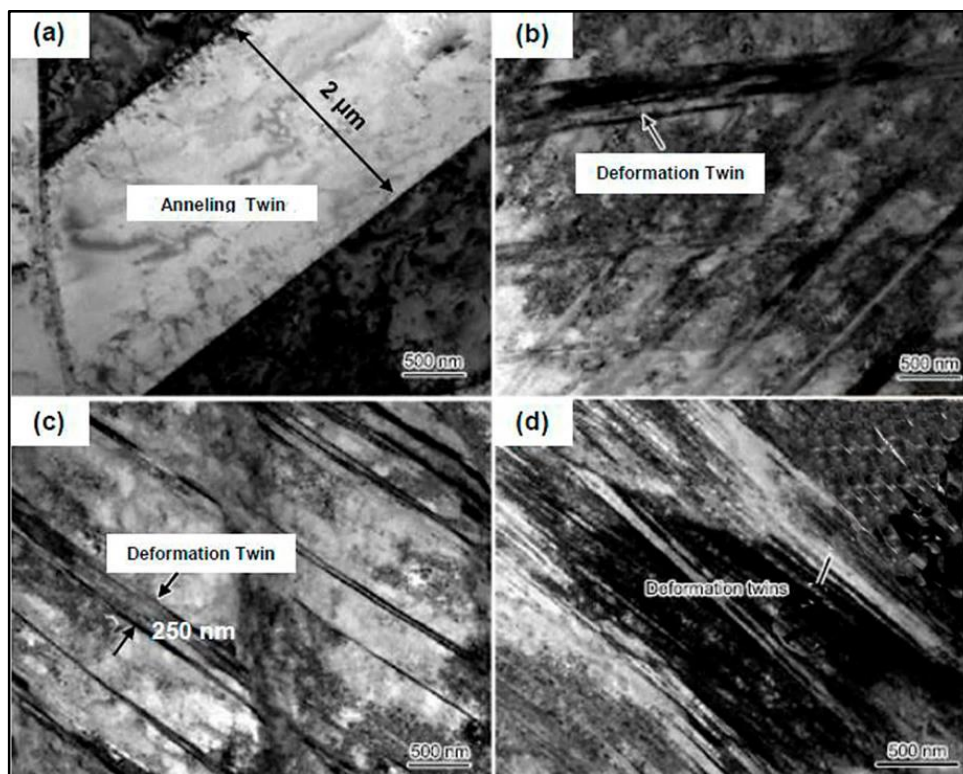

Fig. 15. TEM micrographs of Fe-23%Mn-2%Al-0.2%C steel at different strain rates: (a) un-deformed; (b) $\dot{\varepsilon}=2.97\times10^{-4}s^{-1}$; (c) $\dot{\varepsilon}=2.97\times10^{-3}\,s^{-1}$; (d) $\dot{\varepsilon}=2.97\times10^{-2}\,s^{-1}$

V. MECHANICAL PROPERTIES OF TWIP STEELS

Due to the effect of plasticity induced by twinning, these steels achieve excellent mechanical properties, where high strength and ductility are required. TWIP steels have higher tensile strength and elongation values than other steels used in the automotive industry, as can be seen in Fig. 17 where its advantage is observed. The mechanical properties of typical TWIP steels are reviewed in Fig. 16.
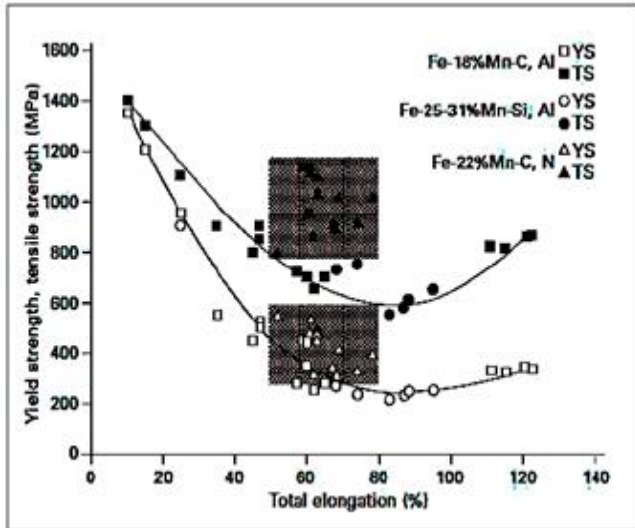

Fig. 16. Typical mechanical properties in medium and high Mn TWIP steels [54].
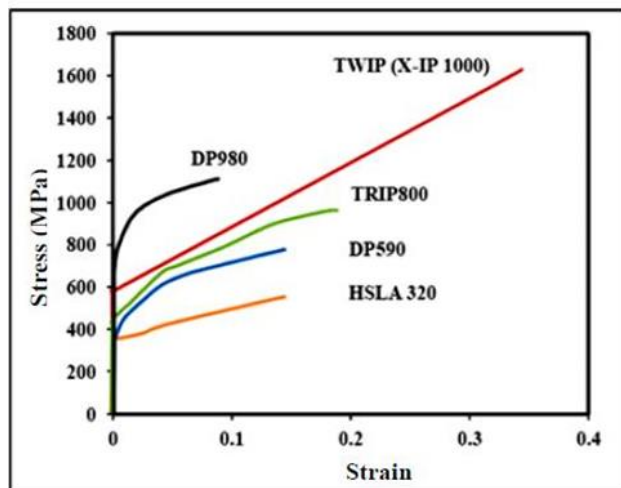

Fig. 17. Stress-strain graphs for a steel TWIP X-IP 1000 and various AHSS steels AHSS [53].

5.1. Yield Stress of TWIP Steels

There are commercial TWIP steels with a tensile strength greater than 1000 MPa and with an elongation greater than 50%, which presents the best combination of resistance-ductility compared to a wide range of steels for automotive applications; but a limiting factor when implementing TWIP steels in the automotive industry is their relatively low yield stress YS; For example, for a Fe-22%Mn-0.6%C industrial

TWIP steel the maximum yield strength is 450-500 MPa [55], while a reasonable value for automobile components is 600-700 MPa. Various ways or strategies have been found to increase the elastic limit which we will briefly describe below.

5.2. Effect of Grain Size on Mechanical Properties

One of the classic strategies to increase the yield stress YS is the refinement of the microstructure of the steel [56]. According to the data obtained by Bouaziz et al. [57], to achieve yield strength values of 600-700 MPa the grain size has to be less than ~ 1μm for a TWIP Fe-22Mn-0.6C steel. Unfortunately, the limitations of the conventional cold rolling industrial process plus subsequent annealing steps limit the size, achieving grain size values slightly above this ideal size.In many publications, it has been shown that the yield strength, YS, of polycrystalline TWIP steels follows the Hall-Petch relationship:

$$\sigma_{ys}(MPa) = \sigma_{ys}^0 + \frac{k_{ys}^{HP}}{\sqrt{d}} \qquad (2)$$

Here, the parameter σ_{YS}^0 includes the lattice frictional stress, the contribution of alloying elements to solid solution hardening, and the contribution to strain hardening of the initial dislocation density, K_{YS}^{HP} it is a material parameter and "d" is the average grain size . Fig. 18 compiles some data showing that TWIP steels obey the Hall-Petch relationship and Table 2 shows the parameters for high Mn TWIP steels and their respective references.
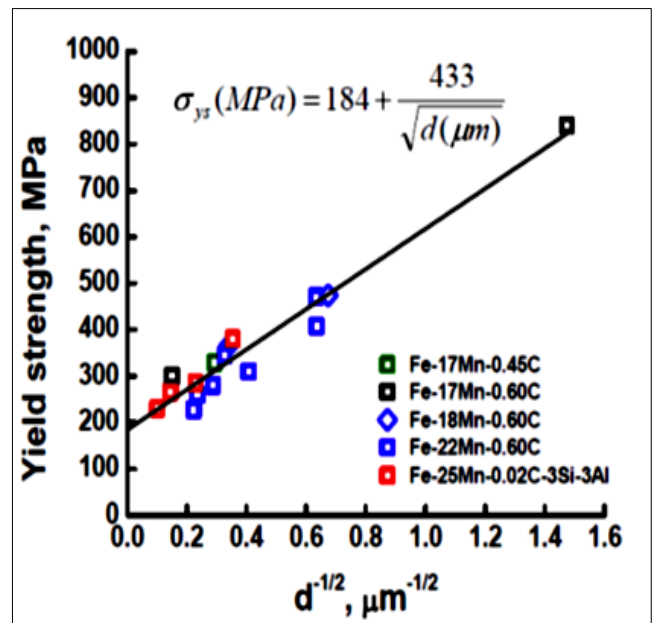

Fig. 18. Verification of the Hall-Petch relation for various TWIP steels (Fe-22%Mn-0.6% C), Fe-17%Mn 0.45%C, Fe-25%Mn-3%Si-3%Al-0.02%C, Fe-17%Mn-0.6%C [58], [59], [60], [61].

Table 2. Parameters of Hall Petch Relation for TWIP Steels

Alloy	σ_{ys}^0 MPa	K_{ys}^{HP} MPaµm$^{1/2}$	Reference
Fe-31%Mn-3%Al-3%Si	53	764	[65]
Fe-22%Mn-0.6%C	137	449	[66]
Fe-22%Mn-0.6C	170	428	[58]
Fe-22%Mn-0.6C	157	357	[67]
Fe-22% Mn-0.5%C-%0.08N	219	478	[44]
Fe-20%Mn—0.6%C	158	485	[68]
Fe-17%Mn—1,5Al-1%Si	208	445	[59]
Fe-15%Mn-0.7%C- 2%Al-2%Si	305	330	[69]

5.3. Pre-deformation by Rolling

Rolling pre-deformation is an interesting strategy for hardening TWIP steels, as it can increase the yield strength significantly. For example, for an Fe-22Mn-0.6C-0.2V steel it has been found that after a reduction of 10%, the yield stress YS increases up to 1000 MPa with elongation values of 25%

5.4 Recovery or partial recrystallization of pre-deformed parts

The pre-deformation of the microstructure, leads to a reduction in ductility. This property could be improved with a restorative or even partial recrystallization treatment after the pre-deformation. It has been observed that for an Fe-22Mn-0.6C steel, an annealing treatment at a temperature below 625ºC results in an interesting combination of yield strength and precipitation hardening. Chateau y col. [62] assumed an increase of 140 MPa in yield stress YS for an Fe-22Mn-0.6C steel due to the precipitation of V carbides. Also, Ding et al, [63] studied the effect of Nb in

TWIP Fe- (20-22) Mn-3Al-3Si steels and concluded that the addition of Nb increases the yield stress of these steels. Similarly, Zamani et al, [64] reported an increase in yield stress for cold rolled and annealed Fe-31Mn-4Si-2Al steel due to the addition of Nb and Ti.

The Hall-Petch diagram, can be affected by alloying additions, as demonstrated in Figure 19 for the case of alloying TWIP steels with Ti, V. It also depends on the pre-strain at which the measurements are taken for a particular material

5.5. Effect of microalloying elements

In TWIP steels, the most widely used microalloying elements are Nb and V. An increase of 200 MPa in yield stress YS has been estimated for a TWIP steel Fe – 21.6Mn – 0.63C – 0.87V due to precipitation hardening of micro alloys.
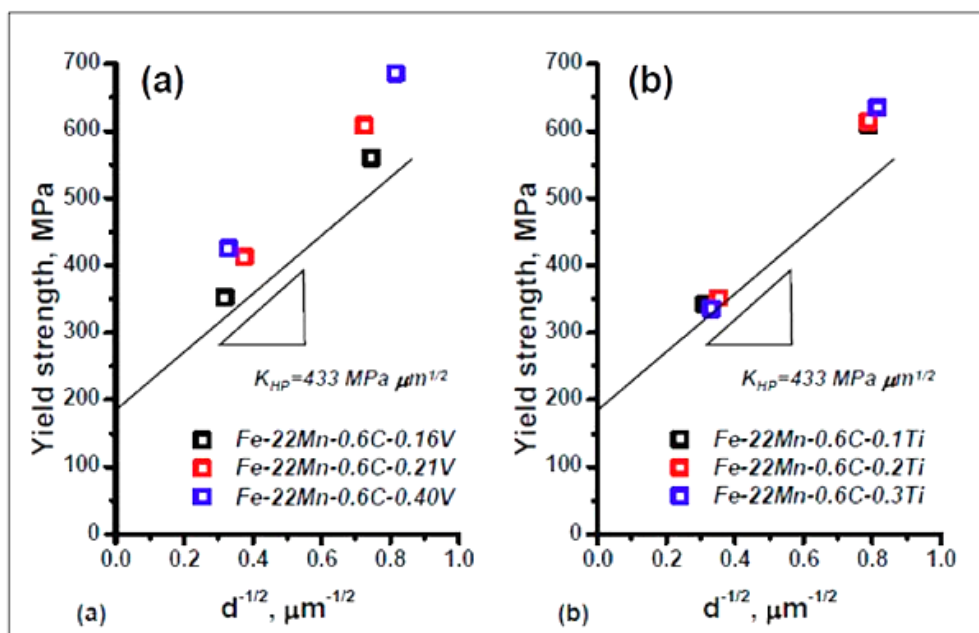

Fig. 19. Influence of micro-alloying additions of (a) V and (b) Ti on the Hall-Petch diagram for TWIP steel [58],[59].
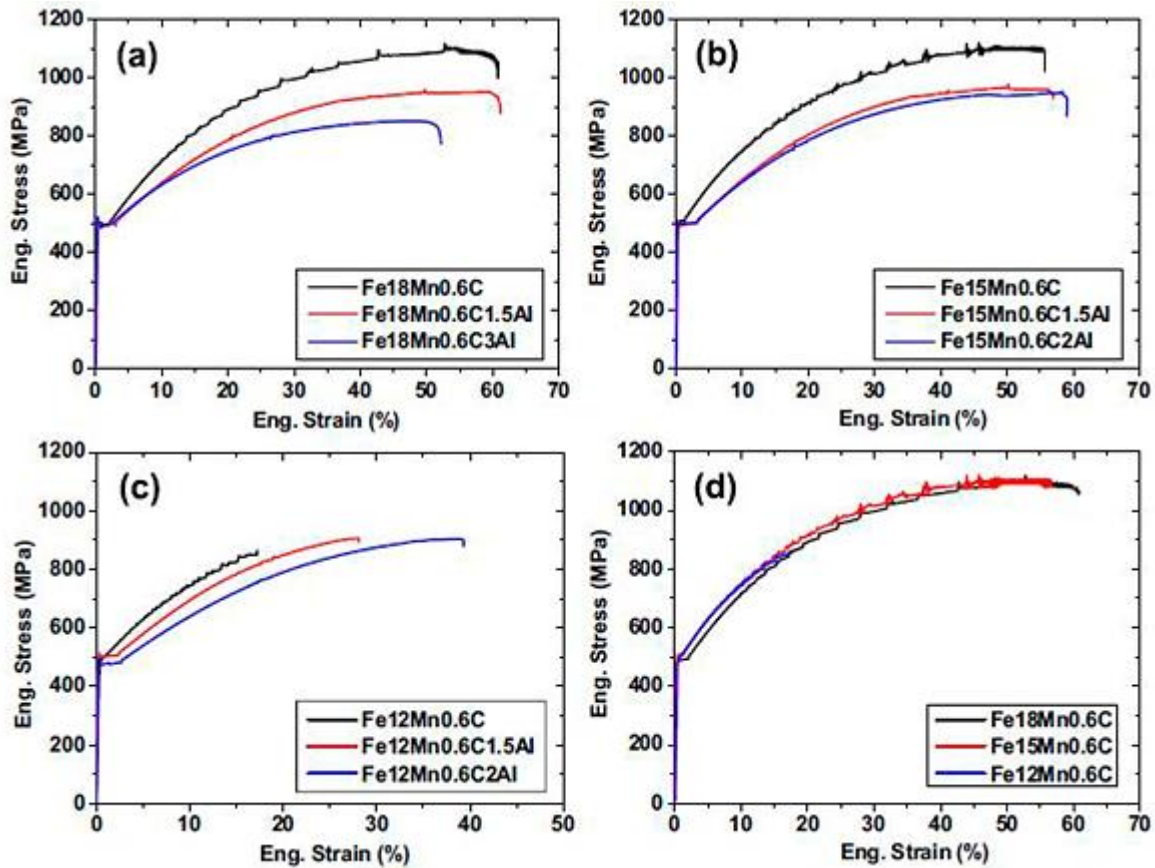
Fig. 20. Comparison of the stress-strain curves of TWIP steels with different Mn and Al compositions, keeping a constant carbon weight percentage (0.6% wt) **[70]**

5.6. Effect of Mn and Al content on Mechanical Properties

All the effects are seen in the graphs in Fig. 20. Thus, in Fig. 20 (a) compares engineering stress-strain curves for Fe-18Mn-0.6C steels with an Al content of 1.5% - 3% by weight. All curves show a yield plateau of 500 MPa. The addition of Al results in a decrease in maximum tensile strength (UTS) and overall elongation. This is a clear indication that Al decreases the work hardening rate because it increases the stacking failure energy SFE. In Figure 20b) the Mn decreases to 15% and the other alloys are almost the same. The curves are very similar. If all the figures are observed together, it is concluded for these cases; that the addition of Al clearly lowers the UTS and greatly increases the total elongation. The effect of Mn on UTS is not pronounced for both Al-free TWIP steels and Al-added steels. The Mn content results in a clear increase in the total elongation of steels without Al and with Al added.

In table 3, the mechanical properties of some TWIP steels with different Mn and Al contents can be observed. It can be seen that FeMn0.6C steel has YS = 484.3 MPa and UTS = 1105.6 MPa; while Fe12Mn0.6C2Al steel has YS = 4776 MPa; UTS = 9146 MPa, the great hardening effect of aluminum is noted at the cost of a drop in ductility from 60.4% to 40.7%

respectively. This drop in ductility may be due to the decrease in Mn content, which directly influences on twinning.

Table 3. Mechanical properties of the some TWIP steels with various Mn and Al content and SFE values **[70]**

Composition (mass %)	YS (MPa)	UTS (MPa)	Total elongation (%)	Critical strain for the onset of serrations (%)	SFE (mJ/m²)
Fe18Mn0.6C	484.1	1105.6	60.4	2.3	14.25
Fe18Mn0.6C1.5Al	498.3	960.1	59.3	18.6	27.53
Fe18Mn0.6C3Al	498.8	848.9	49.7	24.7	40.12
Fe15Mn0.6C	509.3	1124.1	51.3	16	12.38
Fe15Mn0.6C1.5Al	479.5	976.0	57.6	17.1	25.80
Fe15Mn0.6C2Al	488.2	938.9	58.4	18.9	30.12
Fe12Mn0.6C	485.6	837.8	16.1	11	11.84
Fe12Mn0.6C1.5Al	491.9	899.5	30.3	17.5	25.52
Fe12Mn0.6C2Al	477.6	914.6	40.7	16.9	29.86

5.7. Effect of strain rate on the mechanical behavior of TWIP steels

Depending on the alloy system, the mechanical response of TWIP steel differs in strength and elongation and the deformation mechanism varies according to different ranges of strain rate. Wu et al, **[80]** studied the microstructure and mechanical properties of high Mn and low carbon TWIP steel:

Fe18.1% Mn-3.15% Si-3.12% Al-0.03% C during tensile tests in the speed range of deformation of $1.67 \times 10^{-4} - 1 \times 10^{3}$ s^{-1} at room temperature. The results indicated that the inverse effect of the strain rate on the strength of the steel and the strength and ductility of these steels occurred and it also decreased with increasing the strain rate in the quasi-static strain range of

Table 4. Ultimate tensile strength, ultimate elongation and product of strength and ductility of Fe-18.1%Mn-3.15%Si-3.12%Al-0.03%C steel at different strain rates [80].

Strain rate $/s^{-1}$	UTS /MPa	Elongation /%	UTS·Elongation /MPa·%
1.67×10^{-4}	915	55	50325
1.67×10^{-3}	895	55	49225
1.67×10^{-3}	855	45	38475
1.67×10^{-1}	835	45	37575
1.00×10^{1}	850	43	36550
1.00×10^{2}	890	45	40050
1.00×10^{3}	957	56	53592

For a TWIP Fe-23%Mn-2%Al-0.2%C steel, Qin et al. [81] investigated the effect of strain rate on mechanical properties. The results in Fig. 21 show that the strain rate in the range $2.97 \times 10^{-4} - 1.49 \times 10^{-1}$ s^{-1} has no obvious influence on the yield stress YS. However, the tensile strength was slightly reduced and the elongation evidently decreased as the rate of deformation increased.
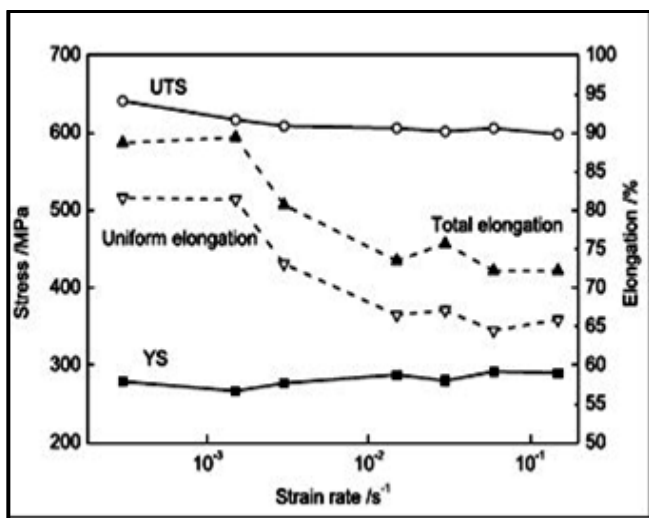

Fig. 21. Mechanical properties of the Fe-23Mn-2Al-0.2C TWIP steel deformed at different strain rates [81]

5.8. Influence of temperature on TWIP steels.

The twinning process does not necessarily play a key role in the strain hardening of TWIP steel. Figure 23 compares the flow curves of TWIP Fe-18% Mn-0.6% C-1.5% Al steel at temperatures in the range -70 °C to + 300 °C. Even though the critical energy SFEγ_{isf} varies over a wide range, from 17 mJ /m^2 at -70°C, up to 82 mJ/m^2, at +300 °C the plasticity of the material remains high, even when aging by Dynamic deformation is very pronounced as can be seen from the jagged flow curves measured in the high temperature range of 100 °C - 300 °C. Since strain twinning is suppressed when γ > 45 mJ /m^2, that is, at +108 °C, these flow curves suggest that strain twins do not necessarily play the most important role in determining the conditions for pronounced strain hardening as observed for TWIP steel.

In most metals, the contribution of twinning to strain increases as temperature is lowered, which can be explained by the fact that the critical twinning stress in most materials increases less rapidly with decreasing temperature. temperature. than yield stress or slip stress flow. On the other hand, The SFE affects the twinning stress [82]; and it alters when the temperature is changed; therefore, a change in the governing deformation mechanism may result. An increase in the strain rate generally results in a greater propensity for twinning [83]. However, under high strain rate strain, a marked increase in temperature, due to adiabatic strain heating, can raise the SFE to or out of the optimal value for twinning, depending on the initial SFE value. The Research carried out by S. Curtze; V. and T. Kuokkala [84] resulted in the graphs presented in Fig. 22. The effect of temperature in three TWIP steels was observed, named: TWIP1: 28% Mn, 1.6% Al; 0.28% Si, 0.08% C: TWIP2: 25% Mn, 1.6% Al, 0.24Si, 0.08% C; TWIP3: 27% Mn, 4.1% Al, 0.52% Si, 0.08% C. As mentioned above, B.C. From Cooman, [47] studied the behavior of TWIP steels of medium and high Mn content, reaching a summary of the mechanical properties (Fig.23)
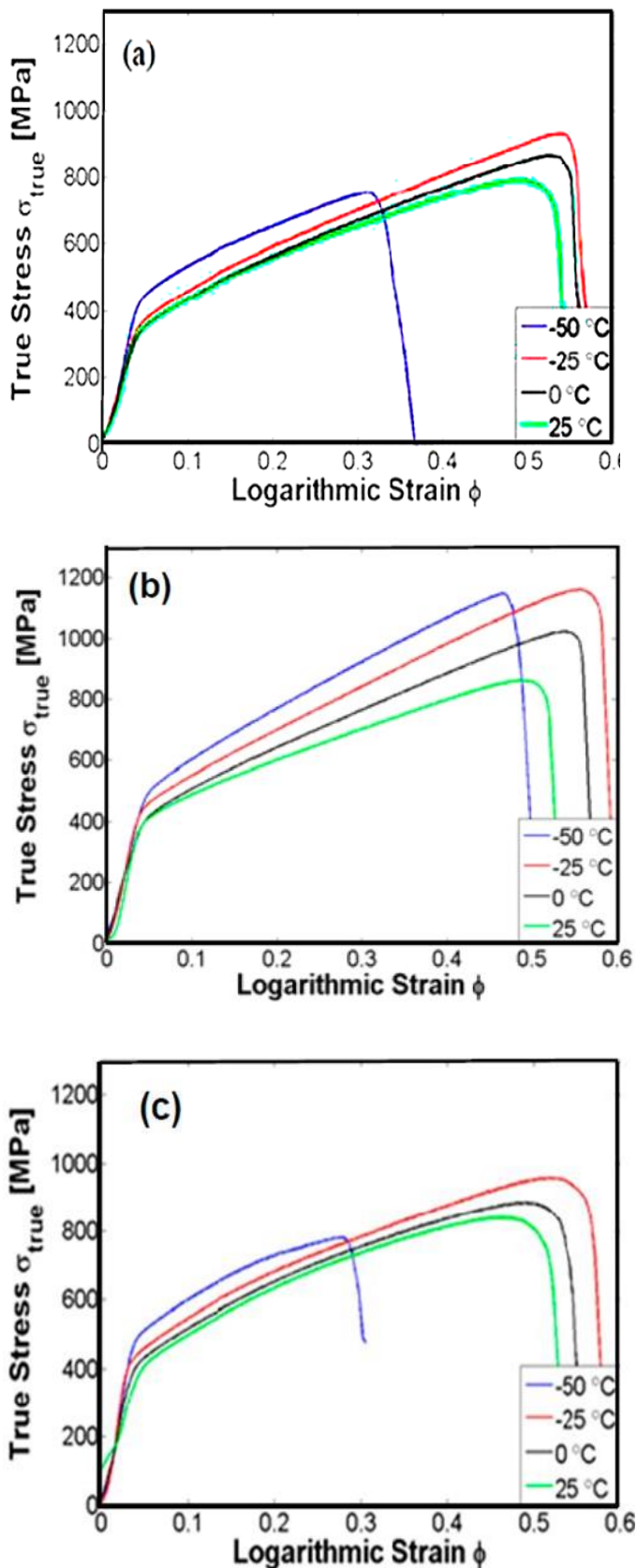
Fig. 23 Engineering stress-strain curves of Fe-18%Mn-0.6%C-1.5%Al TWIP steel in the temperature range of -70°C to +300 °C as measured with a strain rate of 10-3 s-1 [47].

It can be seen; The results obtained in [84] are in close agreement with those obtained in [47], indicating that with an adequate combination of the deformation rate and temperature, they can provide optimal combinations of resistance and ductility; even reaching TWIP steels with a mechanical resistance of 1200 MPa and 60% elongation or 1000MPa with 75% elongation; values that the modern automotive industry demands in its body parts.

VI. CONCLUSIONS

A review of TWIP steels was made, focusing on the mechanisms that explain the mechanical and metallurgical properties of these steels, especially tensile and microstructure mechanical properties. First of all, it is found that there is no standard for the definition of TWIP steels with regard to chemical composition, except for their Mn content, which is in the range (15% - 35%) Mn. The combination of low carbon and high Mn required to suppress strain-induced martensite is clearly defined. However, the border between the alloys is not entirely clear. For example; we have that The addition of Si, Al and Nb have a different influence on the sliding mechanisms due to plastic deformation. The nucleation and growth sites of dislocations and twins are different depending on the type of micro alloys and their percentage by weight.

There is general agreement on the most likely strain hardening mechanisms operating in TWIP steels. These include twinning by deformation and the accumulation of stresses that these cause.

Fig.22. True stress vs. logarithmic strain curves of TWIP steels: (a) TWIP 1 at different temperatures at strain rates of 10^{-3}s^{-1} (b), TWIP 2 at 10^{-3}s^{-1} (c) TWIP 3 at 10^{-3}s^{-1} [84]

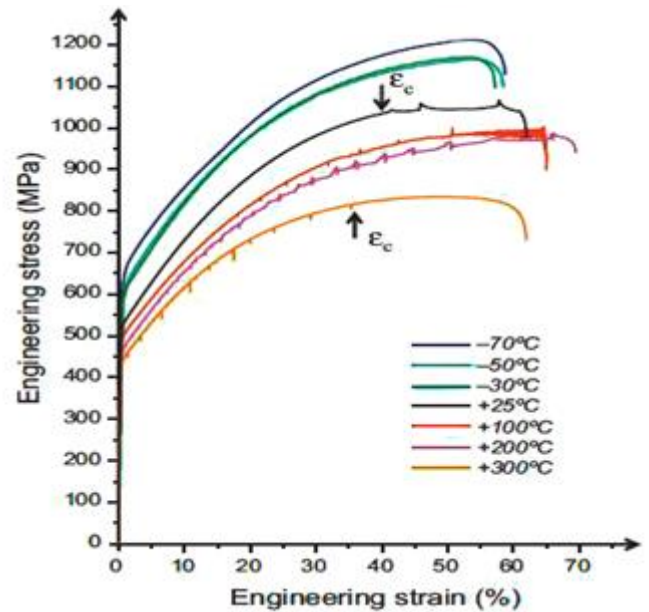However, the magnitude of these mechanisms remains a matter of debate. In certain cases, the quantitative evaluation of the various strain hardening mechanisms remains uncertain.

At present it has become clear; that the TWIP effect is not governed solely by the value of the stacking fault energy (SFE). There are other energy barriers, outlining the pervasive stacking fault energy picture, that also play an essential role. Progress in this area will require a more systematic use of currently available methods and the development of techniques to calculate the SFE of multi-component alloys such as TWIP steels.

The role of carbon in TWIP steels is not entirely clear. Although the ambient temperature diffusion data for Carbon suggest that its influence should be very limited. It is also observed that the tensile mechanical properties depend on many factors such as: the test temperature, deformation speed, chemical composition, grain size and so on; but fundamentally the twinning mechanism is the governing factor.

In summary, this review presents some fundamental aspects of TWIP steels with respect to their alloy design, correlations of mechanical behavior with grain size, strain temperature, strain rate, SFE stacking fault energy and their strain mechanisms.

Despite the fact that numerous studies have been carried out during the last decades; Some efforts still need to be made to have a clear and deep understanding of the relationship between their chemical compositions, microstructures and mechanical properties.

Finally, it can be reported, that the physical metallurgy of TWIP steels is still unclear. Some fundamental research work on the basis of thermodynamic calculations and transformation kinetics is required to obtain a product of higher mechanical strength and elongation with a simple chemical composition system.

.

References

[1] B. C. De Cooman, O. Kwon, K.G. Chin, State-of-the-knowledge on TWIP steel, Mater. Sci. Technol. 28 (5) (2012) 513–527.

[2] O. Bouaziz, S. Allain, C.P. Scott, et al., High manganese austenitic twinning induced plasticity steels: a review of the microstructure properties relationships, Curr. Opin. Solid State Mater. Sci. 15 (4) (2011) 141–168.

[3] J.W. Cho, S. Yoo, M.S. Park, et al., Improvement of Castability and surface quality of continuously cast TWIP slabs by molten mold flux feeding technology, Metall. Mater. Trans. B 48 (1) (2017) 187–196.

[4] O. Grässel, L. Kruger, G. Frommeyer, L. Meyer, Int. J. Plasticity, 16, 2000, 1391

[5] O. Grässel, G. Frommeyer, C. Derder, H. Hofman, J. Phys. IV France, 60, 1997, 383

[6] G. Frommeyer, U. Brux, P. Neumann, ISIJ International, 43, 2003, 438

[7] A. Prakash, T. Hochrainer, E. Reisacher, H. Riedel, Steel Research International, 79, 2008, 645

[8] RAGHAVAN, K. S., SASTRI, A. S. & MARCINKOWSKI, M. J. 1969. Nature of the Work-Hardening Behavior in Hadfield's Manganese Steel. Transactions of the Metallurgical Society of AIME, 245, 1569- 1575

[9] S. E. Kang, J.R. Banerjee, A. Tuling, B. Mintz, Influence of P and N on hot ductility of high Al, boron containing TWIP steels, Mater. Sci. Technol. 11 (2014) 1328–1335.

[10] J.G. Sevillano, An alternative model for the strain hardening of FCC alloys that twin, validated for twinning-induced plasticity steel, Scr. Mater. 60 (2009) 336–339.

[11] M. Dao, L. Lu, Y.F. Shen, S. Suresh, Strength, strain-rate sensitivity and ductility of copper with nanoscale twins, Acta Mater. 54 (2006) 5421–5432.

[12] C.W. Shao, P. Zhang, Y.K. Zhu, Z.J. Zhang, J.C. Pang, Z.F. Zhang, Improvement of low-cycle fatigue resistance in TWIP steel by regulating the grain size and distribution, Acta Mater. 134 (2017) 128–142.

[13] P. Lan, L. Song, C. Du, J. Zhang, Analysis of solidification microstructure and hot ductility of Fe-22Mn-0.7C TWIP steel, Mater. Sci. Technol. 11 (2014) 1297–1304.

[14] O. Bouaziz, S. Allain, C. Scott, P. Cugy, D. Barbier, High manganese austenitic twinning induced plasticity steels: A review of the microstructure properties relationships, Curr. Opin. Solid. St. M. 15 (2011) 141-168.

[15] B.C. De Cooman, O. Kwon, K.-G. Chin, State-of-the-knowledge on TWIP steel, Mater Sci.Tech. 28 (2012) 513-527.

[16] R. Neu, Performance and characterization of TWIP steels for automotive applications, Mater. Perform. Charact. 2 (2013) 244-284.

[17]. ARCELOR Newsletter La actualidad del acero en el automóvil N° 10 - Junio 2005

[18] N.K.Tewary, S.K.Ghosh, Supriya Bera, D.Chakrabarti, S.Chatterjee., Influence of cold rolling on microstructure, texture and mechanical properties of lowcarbon high Mn TWIP steel. Materials Science & Engineering A 615 (2014) 405–415

[19] Z. Mi, D. Tang, L. Yan, J. Guo, High-strength and high-plasticity TWIP steel for modern vehicle, J. Mater. Sci. Technol. 4 (2005) 451–454.

[20] D. Cornette, P. Cugy, A. Hildenbrand, M. Buzekri, Ultra high strength Fe-Mn TWIP steels for automotive safety parts, Metall. Res. Technol. 102 (2005) 905–918.

[21] C. Scott, S. Allain, M.Faral, N.Guelton, Revuede Metallurgie, Cah. Inf. Tech. 103 (2006) 293–302.

[22] O. Grässel, L.Krüger, G.Frommeyer, L.W.Meyer, Int. J.Plasticity16 (2000) 1391–1409.

[23] R. Xiong, R.Fu, Y.Su, Q.Li, X.Wei, L .Li, J. Iron Steel Res. Int.16 (2009) 81.

[24] O. Bouaziz,N.Guelton, Mater. Sci .Eng.:A319–321 (2001)246–249.

[25] G. Dini, A.Najafizadeh, R.Ueji, S.M.Monir-Vaghefi., Mater. Des. 31 (2010) 3395–3402.

[26] J.E. Jin, Y.K.Lee., Mater. Sci . Eng.: A527 (2009) 157–161.

[27] R. Ueji,N. Tsuchida, D.Terada, N.Tsuji, Y.Tanaka, A.Takemura, K. Kunishige, Scr.Mater. 59 (2008) 963–966.

[28] I. Gutierrez-Urrutia ,S.Zaefferer, D.Raabe, Mater .Sci. Eng.: A527 (2010) 3552–3560.

[29] C. Scott, B. Remy, J.L.Collet , A.Cael, C. Bao, F. Danoixd, B. Malardc, C. Curfse, Int. J.Mater. Res. 102 (2011) 538–549.

[30] G. Dini, A.Najafizadeh, R. Ueji, S.M.Monir-Vaghefi, Mater.Lett.64 (2010) 15–18.

[31] J. Gil, "An alternative model for the strain hardening of FCC alloys that twin, validated for twinning-induced plasticity steel," Scr. Mater., vol. 60, no. 5, pp. 336–339, Ma

[32] Y.-K. Lee and C.-S. Choi // Metall. Mater. Trans. A 31 (2000) 355

[33] A. Kelly and K. M. Knowles, Crystallography and Crystal Defects, John Wiley & Sons, Ltd, Chichester, 2nd edn., 2012, ch. 9, pp. 269–304.

[34] Dillamore, I., Butler, E., Green, D., (1968). Crystal rotations under conditions of imposed strain and the influence of twinning and cross-slip. Metal Science Journal, 2 (1), 161-167.

[35] Groves, G., Kelly, A., (1963). Independent slip systems in crystals. Philosophical Magazine, 8 (89), 877-887.

[36] Smallman, R., Green, D., (1964). The dependence of rolling texture on stacking fault energy. Acta Metallurgica, 12 (2), 145-154.

[37] B.C. De Cooman, K.-G. Chin and J.Y. Kim, New Trends and Developments in Automotive System Engineering (InTech, 2011).

[38] Bruno C. De Cooman, Yuri Estrin, Sung Kyu Kim Twinning-induced plasticity (TWIP) steels, Acta Materialia (2017).

[39] Allain, S., Chateau, J. P., Dahamoun, D. and Bouaziz, O., Materials Science and Engineering A, 387-389: 272-276, 2004b.]

[40] Bo Qin, Crystallography of TWIP Steel, A dissertation submitted for the degree of Master of Engineering at Pohang University of Science and Technology, July 2007]

[41] Hull, D. and Bacon, D. J. Introduction to Dislocations, 4th edition, Butterworth-Heinemann, London, 2001.

[42] Bruno C. De Cooman, Yuri Estrin, Sung Kyu Kim, Twinning-Induced Plasticity (TWIP) Steels, Acta Materialia (2017),

doi: 10.1016/j.actamat.2017.06.046]

[43] O. Bouaziz a,b,⇑, S. Allain a, C.P. Scott a,c, P. Cugy a, D. Barbier a High manganese austenitic twinning induced plasticity steels: A review

of the microstructure properties relationships, Current opinion in Solid State and materials Science 15 (2011) 141-168

[44] Bruno C. De Cooman, Yuri Estrin, Sung Kyu Kim, Twinning-Induced Plasticity (TWIP) Steels, Acta Materialia (2017),

doi: 10.1016/j.actamat.2017.06.046]

[45] Dobrzański, L. A., and W. Borek. Thermo-mechanical treatment of Fe–Mn–(Al, Si) TRIP/TWIP steels. Archives of civil and mechanical engineering 2012; 12: 299-304.

[46] Dobrzański L, Grajcar A, Borek W. Microstructure evolution and phase composition of high-manganese austenitic steels. Journal of Achievements in Materials and Manufacturing Engineering 2008; 31:218-25.

[47] B.C. De Cooman, High Mn TWIP steel and medium Mn steel, Graduate Institute of Ferrous Technology, POSTECH, Pohang, South Korea

[48] Cotes S, Sade M, Fernandez-Guillermet A. FCC/HCP martensitic transformation in the Fe-Mn system: Experimental study and thermodynamic analysis of phase stability. Metallurgical and Materials Transactions A 1995;26A

[49] Peng Lan, Jiaquan Zhang, Tensile property and microstructure of Fe-22Mn-0.5C TWIP steel, Materials Science & Engineering A 707 (2017) 373–382

[50] P.S. Kusakin and R.O. Kaibyshev, High-Mn Twinning-Induced Plasticity Steels: microstructure

and mechanical properties, Rev. Adv. Mater. Sci. 44 (2016) 326-360

[51] K.M. Rahmana, V.A. Vorontsova, D. Dyea, The Dynamic Behaviour of a Twinning Induced Plasticity Steel, Materials Science and Engineering A, 2014.

[52] X.M. Qin, L.Q. Chen, W. Deng and H. S. Di, Chin. J. Mater. Res. 25 (2011) 278.

[53] S. Maggi and M. Murgia, "Introduction to the metallurgic characteristics of advanced high-strength steels for automobile applications," Weld. Int., vol. 22.

[54] B. C. De Cooman, Phase transformations in high manganese twinning-induced plasticity (TWIP) steels, Woodhead Publishing Limited, 2012, South Korea.

[55] H. W. Yen, M. Huang, C. P. Scott, and J. R. Yang, "Interactions between deformation-induced defects and carbides in a vanadium-containing TWIP steel," Scr. Mater., vol. 66, no. 12, pp. 1018–1023, Jun. 2012.

[56] G. E. Totten, "Steel heat treatment-Metallurgy and technologies," Ed. CRC Press, 2006.

[57] O. Bouaziz, S. Allain, C. P. Scott, P. Cugy, and D. Barbier, "High manganese austenitic twinning induced plasticity steels: A review of the microstructure properties relationships," Curr. Opin. Solid State Mater. Sci., vol. 15, no. 4, pp. 141–168, 2011.

[58] C. Scott, B. Remy, J.-L. Collet, A. Cael, C. Bao, F. Danoix, B. Malard, C. Curfs, Precipitation strengthening in high manganese austenitic TWIP steels, Int. J. Mater. Res. 102 (2011) 538 -549.

[59] H. Gwon, MS Thesis, Pohang University of Science and Technology, South Korea, 2017.

[60] S.-H. Wang, Z.-Y. Liu, G.-F. Wang, Influence of grain size on TWIP effect in a TWIP steel, Acta Mater. Sin. 45 (2009) 1083

[61] H.-W. Yen, M. Huang, C. Scott, J.-R. Yang, Interactions between deformation induced defects and carbides in a vanadium-containing TWIP steel, Scr. Mater 66 (2012) 1018-1023.

[62] J. P. Chateau, A. Dumay, S. Allain, and A. Jacques, "Precipitation hardening of a FeMnC TWIP steel by vanadium carbides," J. Phys. Conf. Ser., vol. 240, Jul. 2010.

[63] H. Ding, H. Li, H. Ding, C. Qiu, and Z. Tang, "Partial inverse grain size dependence of strength in high Mn steels microalloyed with Nb," J. Iron Steel Res. Int., vol. 9, no. 2009001, pp. 68–72, 2012.

[64] D. Zamani, A. Najafizadeh, and G. R. Razavi, "Effect of Thermo-Mechanical Treatment on Mechanical Properties and Microstructure of Fe-31Mn-4Si-2Al-Nb- Ti TWIP Steel," Int. Conf. Adv. Mater. Eng., vol. 15, pp. 45–49, 2011.

[65] G. Dini, A. Najafizadeh, R. Ueji, S. Monir-Vaghefi, Tensile deformation behavior of high manganese austenitic steel: the role of grain size, Mater, Des 31 (2010) 3395-3402.

[66] O. Bouaziz, S. Allain, C. Scott, P. Cugy, D. Barbier, High manganese austenitic twinning induced plasticity steels: a review of the microstructure properties relationships, Curr. Opin. Solid. St. M. 15 (2011) 141-168

[67] J.G. Sevillano, F. de Las Cuevas, Internal stresses and the mechanism of work hardening in twinning-induced plasticity steels, Scr. Mater 66 (2012) 978-981.

[68] Y. Shen, N. Jia, R. Misra, L. Zuo, Softening behavior by excessive twinning and adiabatic heating at high strain rate in a Fe-20Mn-0.6 C TWIP steel, Acta Mater 103 (2016) 229-242

[69] K. Rahman, V. Vorontsov, D. Dye, The effect of grain size on the twin initiation stress in a TWIP steel, Acta Mater 89 (2015) 247- 257.

[70] Jin-KyungKim,, Bruno C.De Cooman, Stacking fault energy and deformation mechanisms in Fe-xMn-0.6C-yAl TWIP steel, Materials Science & Engineering A 676 (2016) 216–231]

[71] G. Frommeyer , U. Brüx , P. Neuman // ISIJ Int. 43 (2003) 438…71

[72] S. Allain, J.P. Chateau, O. Bouaziz, S. Migot, N. Guelton // Mater. Sci. Eng: A 387-389 (2004) 158.

[73] S. Allain, J.-P. Chateau, O. Bouaziz, S. Migot, and N. Guelton, "Correlations between the calculated stacking fault energy and the plasticity mechanisms in Fe– Mn–C alloys," Mater. Sci. Eng. A, vol. 387–389, pp. 158–162, Dec. 2004.

[74] A. Asghari, A. Zarei-Hanzaki, and M. Eskandari, "Temperature dependence of plastic deformation mechanisms in a modified transformation-twinning induced plasticity steel," Mater. Sci. Eng. A, vol. 579, pp. 150–156, Sep. 2013.

[75] A. Dumay, J.-P. Chateau, S. Allain, S. Migot, and O. Bouaziz, "Influence of addition elements on the stacking-fault energy and mechanical properties of an austenitic Fe–Mn–C steel," Mater. Sci. Eng. A, vol. 483–484, pp. 184–187, Jun. 2008.

[76] K. Sato, M. Ichinose, Y. Hirotsu et al., ISIJ Int. 29 (1989) p.868.

[77] J.W. Christian and S. Mahajan, Prog. Mater. Sci. 39 (1995) p.1.

[78] Y.F. Shen, Y.D.Wang , X.P. Liu, X. Sun b, Lin Peng , S.Y. Zhang, L. Zuo , P.K. Liaw., Deformation mechanisms of a 20Mn TWIP steel investigated by in situ neutron diffraction and TEM , Acta Mater (2013),

http://dx.doi.org/10.1016/j.actamat.2013.06.051

[79] Christian J, Mahajan S. Deformation twinning. Progress in Materials Science 1995;39:1

[80] Z.Q. Wu, Z.Y. Tang, H.Y. Li and H.D. Zhang, Acta Metall. Sin. 48 (2012) 593.

[81] X.M. Qin, L.Q. Chen, W. Deng and H. S. Di, Chin. J. Mater. Res. 25 (2011) 278.

[82] J.A. Venables, "Deformation twinning in face-centred cubic metals", Philosophical Magazine, v. 6, pp. 379, 1961.

[83] Christian, J.W., Mahajan, S., "Deformation Twinning", Progress in Materials Science, v. 39, n. 1-2, pp. 1-157, 1995.

[84] S. Curtze; V.-T. Kuokkala, Effects of temperature and strain rate on the tensile properties of TWIP steels, Revista Matéria, v. 15, n. 2, pp. 157-163, 2010.